DATA ANALYTICS AND APPLIED MATHEMATICS (DAAM)
e-ISSN: 2773-4854
VOL. 2, ISSUE 1, 011 – 019
DOI: https://doi.org/10.15282/daam.v2i1.6431

ORIGINAL ARTICLE

Boundary layer flow on permeable flat surface in Ag-Al_2O_3/Water hybrid nanofluid with viscous dissipation

M.K.A. Mohamed[1,*], A. Hussanan[2], H.T. Alkasasbeh[3], B. Widodo[4] and M.Z. Salleh[1]

[1]Centre for Mathematical Sciences, College of Computing and Applied Sciences, Universiti Malaysia Pahang, Lebuhraya Tun Razak, 26300 Gambang, Kuantan, Pahang, Malaysia.
[2]Department of Mathematics, Division of Science and Technology, University of Education, Lahore, 54000, Pakistan.
[3]Department of Mathematics, Faculty of Science, Ajloun National University, P.O. Box 43, Ajloun 26810, Jordan.
[4]Department of Mathematics, Institut Teknologi Sepuluh Nopember, 60111 Surabaya, Indonesia.

ABSTRACT – Seeking the better performance nanofluid but with low cost of production, presence challenged. Metal nanomaterial is good in both thermal and electric conductivity but expensive while oxide nanomaterial does oppositely. The present study solved numerically the laminar boundary layer flow over a permeable flat surface in a blended metal-oxide hybrid nanofluid plate with viscous dissipation effects. The similarity equations in the form of the set of ordinary differential equations are reduced from the non-linear partial differential equations before being solved numerically using the Runge-Kutta-Fehlberg method in MAPLE. The numerical solution is obtained for the reduced skin friction coefficient and reduced Nusselt number as well as the temperature and velocity profiles. The flow features and the heat transfer characteristic for the Eckert number, permeability parameter and nanoparticle volume fraction are analyzed and discussed. The Ag-Al_2O_3 water-based hybrid nanofluid tested in this study shows competitive results with the Ag water-based nanofluid in certain cases.

ARTICLE HISTORY
Received: 07/05/2021
Revised: 25/06/2021
Accepted: 29/06/2021

KEYWORDS
Boundary layer
Hybrid nanofluid
Suction/injection effect
Viscous dissipation

INTRODUCTION

Common industrial application applied fluid engineering in heat transfer management system. The convective heat transfer process is everywhere starting from the refrigerator in the kitchen, air-conditioner in the living room, engine oil, radiator as an engine cooling system, until at the tyre production plant to cool the end product [1]. Revolution from the use of based fluid like water and oil to nanofluid is an important achievement in fluid engineering. The presence of nanomaterial in the fluid has drastically enhanced the fluid flow and heat transfer characteristics, due to its high thermal conductivity like silver and gold. Of course, the use of this premium metal are not suitable for low-cost applications thus there is a gap in improving the fluid performance and cost [2]. Industries need fluid with good heat transfer performance but cheap.

This study implements the use of hybrid nanofluid in the convective heat transfer process over a permeable flat surface with viscous dissipation effects. Previous studies on boundary layer flow over nanofluid include the works of [3], [4], [5], [6], and recently by [7], [8] and [9].

The laminar flow on a flat plate is first studied by [10]. As Blasius investigated the static flat plate with moving flow, [11] proposed a study of a moving plate with the static flow. Although the Navier stokes equation is identical for both problem, it is distinguished by the boundary conditions of fluid [12]. Known as Blasius and Sakidis flow respectively, the study of boundary layer flow over a flat surface has been investigated with a Newtonian and non-Newtonian fluid like the micropolar fluid by [13], the nanofluid by [14] and [15], the Casson fluid by [16] and the ferrofluid by [17] and [18], respectively.

Next, [19] considers the convective surface boundary conditions on the Blasius flow then extended by [20] with a suction and injection effect. Both investigations employed the RKF45 as the numerical method. The recent study includes the works from [21], [22], [23], [24] and [25] who extend the Blasius model with thermal radiation effect, heat absorption, chemical reaction, viscous dissipation effect, the slip effect, suction/injection effect and convective boundary conditions, respectively.

The present study considered the steady convective heat transfer and boundary layer flow over a permeable flat surface in Ag-Al_2O_3 water-based hybrid nanofluid plate with viscous dissipation effects. Viscous dissipation effects are significant in temperature rising in polymer processing flow such as injection modelling or extrusion at high rates. It is also usually present from large deceleration from high rotating speeds [26]. Next, the Alumina Al_2O_3 is oxide nanoparticles with low density and its cheap while silver Ag has great thermal conductivity. Blending both nanoparticles in this study is expected to provide the theoretical knowledge for the hybrid nanofluid flow over a permeable surface, therefore provided the

*CORRESPONDING AUTHOR | M.K.A. Mohamed | ✉ mkhairulanuar@ump.edu.my

preliminary data that described the fluid parameter effects on the characteristic of fluid flow. Based on the literature studies, this topic is never been consider by anyone previously, thus the results provided from this investigation are new.

MATHEMATICAL FORMULATION

Figure 1 shows an *Ag-Al₂O₃/Water* hybrid nanofluid flow over a flat surface with ambient temperature T_∞ and free stream velocity U_∞. u and v is assumes as the velocity components along a direction of x and y axes, respectively. Next, the surface temperature and the permeability of the plate is denoted as T_w and v_w. Assuming the pressure in the boundary layer is constant along x-direction, the boundary layer equations and heat transfer that can be governed are:

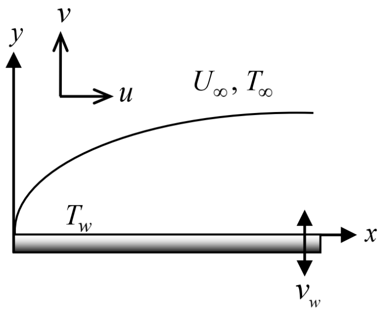

Figure 1. Boundary layer flow over a flat surface with suction/injection effect.

$$\frac{\partial u}{\partial x}+\frac{\partial v}{\partial y}=0, \tag{1}$$

$$u\frac{\partial u}{\partial x}+v\frac{\partial u}{\partial y}=v_{hnf}\frac{\partial^2 u}{\partial y^2}, \tag{2}$$

$$u\frac{\partial T}{\partial x}+v\frac{\partial T}{\partial y}=\frac{k_{hnf}}{\left(\rho C_p\right)_{hnf}}\frac{\partial^2 T}{\partial y^2}+\frac{\mu_{hnf}}{\left(\rho C_p\right)_{hnf}}\left(\frac{\partial u}{\partial y}\right)^2, \tag{3}$$

with

$$\begin{gathered} u=0,\quad v=v_w,\quad T=T_w \text{ at } y=0,\\ u\to U_\infty,\quad T\to T_\infty, \text{ as } y\to\infty. \end{gathered} \tag{4}$$

where T is the temperature in the boundary layer while v_{hnf}, $\mu_{hnf}, k_{hnf}, \rho_{hnf}$ and $\left(\rho C_p\right)_{hnf}$ are the hybrid nanofluid kinematic viscosity, the dynamic viscosity, the thermal conductivity, the density and the heat capacity, respectively. Other properties related to water based-fluid and the nanoparticles are denoted with subscript $_f$ and $_{s1,s2}$ respectively as follows [2]:

$$\begin{gathered} v_{hnf}=\frac{\mu_{hnf}}{\rho_{hnf}},\quad \rho_{hnf}=(1-\phi_2)\left[(1-\phi_1)\rho_f+\phi_1\rho_{s1}\right]+\phi_2\rho_{s2},\quad \mu_{hnf}=\frac{\mu_f}{(1-\phi_1)^{2.5}(1-\phi_2)^{2.5}},\\ \left(\rho C_p\right)_{hnf}=(1-\phi_2)\left[(1-\phi_1)\left(\rho C_p\right)_f+\phi_1\left(\rho C_p\right)_{s1}\right]+\phi_2\left(\rho C_p\right)_{s2},\\ \frac{k_{hnf}}{k_{bf}}=\frac{k_{s2}+2k_{bf}-2\phi_2(k_{bf}-k_{s2})}{k_{s2}+2k_{bf}+\phi_2(k_{bf}-k_{s2})},\quad \frac{k_{bf}}{k_f}=\frac{k_{s1}+2k_f-2\phi_1(k_f-k_{s1})}{k_{s1}+2k_f+\phi_1(k_f-k_{s1})} \end{gathered} \tag{5}$$

where ϕ_1, ϕ_2 are nanoparticles volume fraction for silver *Ag* and alumina *Al₂O₃*, respectively. The values of thermophysical properties of water and nanoparticles consider are tabulated in Table 1. The governing equations (1)-(3) are dimensional with many dependent variables thus possess difficulties in solving. Therefore, the similarity variables η is used to eliminate the dependent variables as well as it independent variable.

$$\eta=\left(\frac{U_\infty}{vx}\right)^{1/2}y,\quad \psi=\left(U_\infty vx\right)^{1/2}f(\eta),\quad \theta(\eta)=\frac{T-T_\infty}{T_w-T_\infty}, \tag{6}$$

Noticed that, the equation (1) is satisfied by the (6) with

$$u = \frac{\partial \psi}{\partial y} \text{ and } v = -\frac{\partial \psi}{\partial x}. \tag{7}$$

ψ is the non-dimensional stream function while θ is the non-dimensional temperature. Using (6) and (7), the equation (2) and (3) is transformed to a more convenience way as:

$$\frac{\nu_{hnf}}{\nu_f} f''' + \frac{1}{2} ff'' = 0 \tag{8}$$

$$\frac{1}{\Pr}\frac{k_{hnf}}{k_f}\frac{(\rho C_p)_f}{(\rho C_p)_{hnf}}\theta'' + \frac{1}{2} f\theta' + \frac{\nu_{hnf}}{\nu_f}\frac{\rho_{hnf}\left(C_p\right)_f}{\left(\rho C_p\right)_{hnf}} Ec\, f'' = 0. \tag{9}$$

By definition, $\Pr = \dfrac{\nu_f\left(\rho C_p\right)_f}{k_f}$ is a Prandtl number. In this study, water is assigned as the based-fluid, thus Pr is set as 6.2. Further, $Ec = \dfrac{(U_\infty)^2}{C_p(T_w - T_\infty)}$ is an Eckert number. Other quantities related to hybrid nanofluid are as follows:

$$\frac{\nu_{hnf}}{\nu_f} = \frac{1}{(1-\phi_1)^{2.5}(1-\phi_2)^{2.5}\left[(1-\phi_2)+\left[(1-\phi_1)+\phi_1(\rho_{s1}/\rho_f)\right]+\phi_2(\rho_{s2}/\rho_f)\right]},$$

$$\frac{(\rho C_p)_f}{(\rho C_p)_{hnf}} = \frac{1}{(1-\phi_2)\left[(1-\phi_1)+\phi_1(\rho C_p)_{s1}/(\rho C_p)_f\right]+\phi_2(\rho C_p)_{s2}/(\rho C_p)_f},$$

$$\frac{\rho_{hnf}\left(C_p\right)_f}{\left(\rho C_p\right)_{hnf}} = \frac{(1-\phi_2)\left[(1-\phi_1)\rho_f+\phi_1\rho_{s1}\right]+\phi_2\rho_{s2}}{(1-\phi_2)\left[(1-\phi_1)\rho_f+\phi_1\left(\rho C_p\right)_{s1}/\left(C_p\right)_f\right]+\phi_2\left(\rho C_p\right)_{s2}/\left(C_p\right)_f}.$$

In order that the similarity solution for equations (1) to (4) exist, let [20]:

$$v_w = -\left(\frac{U_\infty \nu_f}{4x}\right)^{1/2}\lambda \tag{10}$$

where λ is permeability rate at the plate surface constant. $\lambda > 0$ corresponds for suction effects while $\lambda < 0$ corresponds the injection effects. The boundary conditions (4) becomes

$$\begin{gathered} f(0) = \lambda,\ f'(0) = 0,\ \theta(0) = 1, \\ f'(\eta) \to 1,\ \theta(\eta) \to 0,\ \text{as } y \to \infty. \end{gathered} \tag{11}$$

The values of $f''(0)$ and $-\theta'(0)$ obtained from the numerical computation are transformed to a reduced skin friction coefficient $C_f \operatorname{Re}_x^{1/2}$ and reduced Nusselt number $Nu_x \operatorname{Re}_x^{-1/2}$ defined as

$$C_f \operatorname{Re}_x^{1/2} = \frac{f''(0)}{(1-\phi_1)^{2.5}(1-\phi_2)^{2.5}} \text{ and } Nu_x \operatorname{Re}_x^{-1/2} = -\frac{k_{hnf}}{k_f}\theta'(0) \tag{12}$$

where

$$C_f = \frac{\tau_w}{\rho_f u_\infty^2},\quad Nu_x = \frac{x q_w}{k_f(T_w - T_\infty)},\quad \tau_w = \mu_{hnf}\left(\frac{\partial \bar{u}}{\partial \bar{y}}\right)_{\bar{y}=0},\quad q_w = -k_{hnf}\left(\frac{\partial T}{\partial \bar{y}}\right)_{\bar{y}=0},\quad \operatorname{Re}_x = \frac{U_\infty x}{\nu_f} \tag{13}$$

is the local skin friction coefficient, the Nusselt number, the surface shear stress, the surface heat flux and the Reynolds number, respectively.

RESULTS AND DISCUSSION

The transformed equations (8) and (9) with (10) are solved numerically using the Runge-Kutta-Fehlberg in MAPLE. Also known as RKF45, this method implements a 4th order approximation with an error estimator of order 5. Mathematically, the approximation is determined by adding the present value with the weighted average of four increments.

From the numerical computation, the boundary layer thickness is set from 7 to 11 to provide the asymptotic temperature and velocity profiles. The asymptotic feature is the characteristics that the numerical computation run in this study is free from the influence of boundary layer thickness values set, thus produced the precise results. The numerical results obtained for the reduced Nusselt number $Nu_x \mathrm{Re}_x^{-1/2}$ and the reduced skin friction coefficient $C_f \mathrm{Re}_x^{1/2}$ for various values of permeability parameter λ, Eckert number Ec and the nanoparticle volume fraction for alumina Al_2O_3 (ϕ_1) and silver $Ag(\phi_2)$. In order to validated the efficiency numerical method and mathematical formulation used, the comparison results with previously studied have been done. Table 2 shows the comparison results with the previously published results for viscous fluid and Al_2O_3 / $Water$ nanofluid by [10] and [27], respectively. It is concluded that the results are in good agreement thus gives confidence to the precision for the overall results shows in this study.

Table 1. Thermophysical properties of water and nanoparticles.

Physical Properties	Water (*f*)	Al_2O_3 (ϕ_1)	$Ag(\phi_2)$
ρ (kg/m^3)	997	3970	10500
C_p (J/kg·K)	4179	765	235
k(W/m·K)	0.613	40	429

Table 2. Comparison values of $C_f \mathrm{Re}_x^{1/2}$ for some values of ϕ_1 for Al_2O_3 / $Water$ nanofluid when $Ec = \lambda = \phi_2 = 0$, and $\Pr = 6.2$,

ϕ_1	Blasius [10]	Ahmad et al. [27]	Present
0	0.3321	0.3321	0.33205
0.002		0.3339	0.33388
0.004		0.3357	0.33571
0.008		0.3394	0.33939
0.1		0.3412	0.34123
0.2		0.3506	0.35056
0.1		0.4316	0.43161
0.2		0.5545	0.55451

Next, Figures 2-5 shows the temperature profiles $\theta(\eta)$ and velocity profiles $f'(\eta)$ for various values of permeability parameter λ and viscous dissipation parameter known as Eckert number *Ec*, respectively. From the temperature profiles in Figures 2 and 3, it is found that the presence of viscous dissipation effect, *Ec* and the injection on plate $(\lambda < 0)$ results in the increase of thermal boundary layer thickness. Thermal dispersion in a boundary layer increases as the viscous dissipation presence, thus extend the thickness of the boundary layer. The suction effect $(\lambda > 0)$ on the other hand reduced the thermal boundary layer thickness, thus results in the increase in temperature gradient which represent by the Nusselt number.

From Figure 4, it is observed that the various values of *Ec* did not gave any effects on the velocity profiles. Physically, the viscous dissipation effects represented by Ec is the converting process of induced kinetic energy into thermal energy [28]. This provided information that the velocity boundary layer thickness, the velocity gradient or skin friction coefficient is not affected by the viscous dissipation effects. In Figure 5, the injection effect $(\lambda < 0)$ enhanced the velocity boundary layer thicknesses, while the suction effect $(\lambda > 0)$ does contrary. The suction effect has reduced the fluid flow dispersion by attracting the fluid particle through the permeable plate thus reduced the velocity boundary layer thicknesses. Physically, increasing fluid particle on the plate results from suction effects has influenced the increase in the skin friction between the fluid and the plate surface.

The distribution of reduced Nusselt number $Nu_x \mathrm{Re}_x^{-1/2}$ with various values of λ and *Ec* are illustrated in Figures 6 and 7. Four types of fluid are considered which are the water-based fluid $(\phi_1 = \phi_2 = 0)$, the 0.1 vol. Al_2O_3 / $Water$ nanofluid $(\phi_1 = 0.1, \phi_2 = 0)$, the 0.16 vol. $Ag - Al_2O_3$ / $Water$ hybrid nanofluid $(\phi_1 = 0.1, \phi_2 = 0.06)$ and the 0.16 vol. Ag / $Water$ nanofluid. Specifically Ag / $Water$ nanofluid blend from metal type nanoparticles Ag with high density and thermal conductivity. Besides, it is also expensive. From Figure 6, as $Ec = 0$, the Ag / $Water$ nanofluid scored highest in $Nu_x \mathrm{Re}_x^{-1/2}$ closely followed by 0.16 vol. $Ag - Al_2O_3$ / $Water$ hybrid nanofluid. The water-based fluid scored lowest which reflect weak convective heat transfer capability compared to other nanofluids. As $Ec > 0$, it is observed that the Ag / $Water$ nanofluid has the most drastical reduction in $Nu_x \mathrm{Re}_x^{-1/2}$. The Nusselt number reduced nearly to 0

$\left(Nu_x \,\mathrm{Re}_x^{-1/2}\ ;\ 0\right)$ compared to the other fluid. Physically, the high values of Ec reduct the convective heat transfer capability thus promote the conduction heat transfer. It is realistic for $Ag\,/\,Water$ nanofluid since the Ag nanoparticle thermal conductivity is the highest compared to other nanoparticle tested.

In Figure 7, it is found that the values of $Nu_x \,\mathrm{Re}_x^{-1/2}$ for 0.16 vol. $Ag - Al_2O_3\,/\,Water$ hybrid nanofluid and $Ag\,/\,Water$ nanofluid are competitive as suction/injection effect is not presence $(\lambda = 0)$, while the values of $Nu_x \,\mathrm{Re}_x^{-1/2}$ for water-based fluid is the lowest. As the presence of suction effect $(\lambda > 0)$, the values of $Nu_x \,\mathrm{Re}_x^{-1/2}$ increases for all fluid and dominates by the water-based fluid while the $Ag\,/\,Water$ nanofluid scored the lowest $Nu_x \,\mathrm{Re}_x^{-1/2}$ values.

Lastly, a distribution variation of $C_f \,\mathrm{Re}_x^{1/2}$ for various values of λ is shown in Figure 8. From the figure, it is found that the presence of injection effect $(\lambda < 0)$, has reduced the values of $C_f \,\mathrm{Re}_x^{1/2}$. The trends are contrary for suction effect $(\lambda > 0)$. The increase of λ raise the skin friction coefficient. The increase of nanoparticle in fluid as well as the higher density of nanoparticle have contributed to the increase of a skin friction coefficient. It is clearly shown in Figure 8 where the $Ag\,/\,Water$ nanofluid scored highest in $C_f \,\mathrm{Re}_x^{1/2}$ followed by the 0.16 vol. $Ag - Al_2O_3\,/\,Water$ hybrid nanofluid.

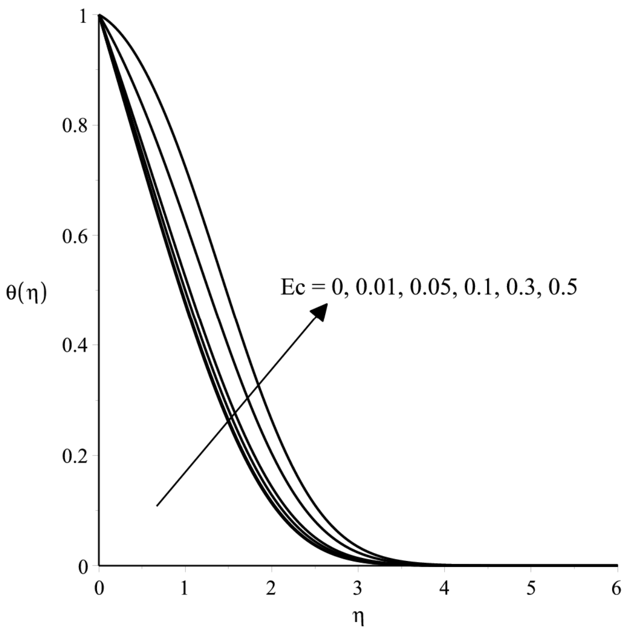

Figure 2. Temperature profiles $\theta(\eta)$ for Ec when $\mathrm{Pr} = 6.2,\ \phi_1 = 0.1,\ \phi_2 = 0.06$ and $\lambda = 0$.

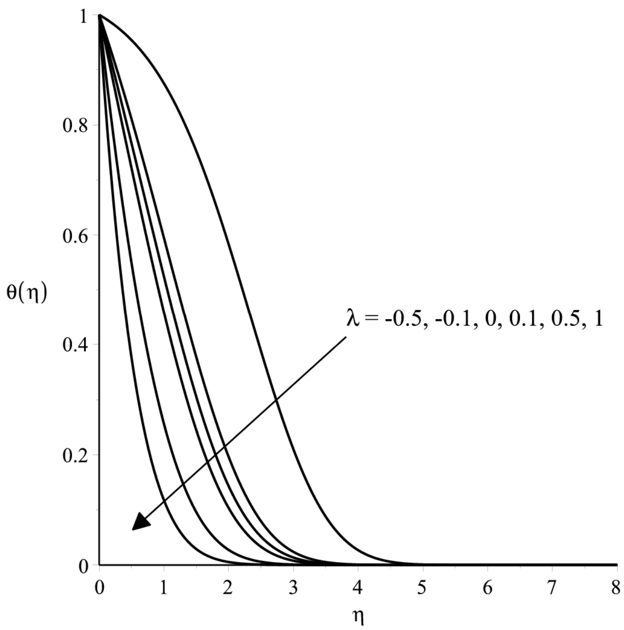

Figure 3. Temperature profiles $\theta(\eta)$ for λ when $Ec = \phi_1 = 0.1,\ \phi_2 = 0.06$ and $\mathrm{Pr} = 6.2$.

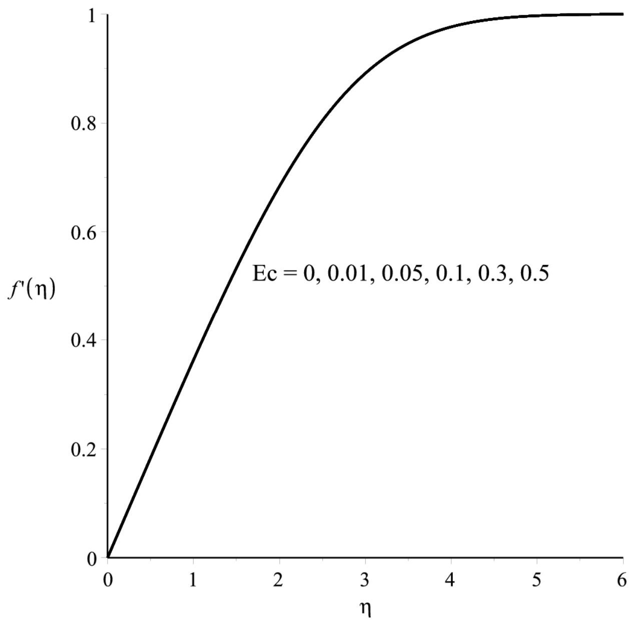

Figure 4. Velocity profiles $f'(\eta)$ for Ec when $\Pr = 6.2,\ \phi_1 = 0.1,\ \phi_2 = 0.06$ and $\lambda = 0$.

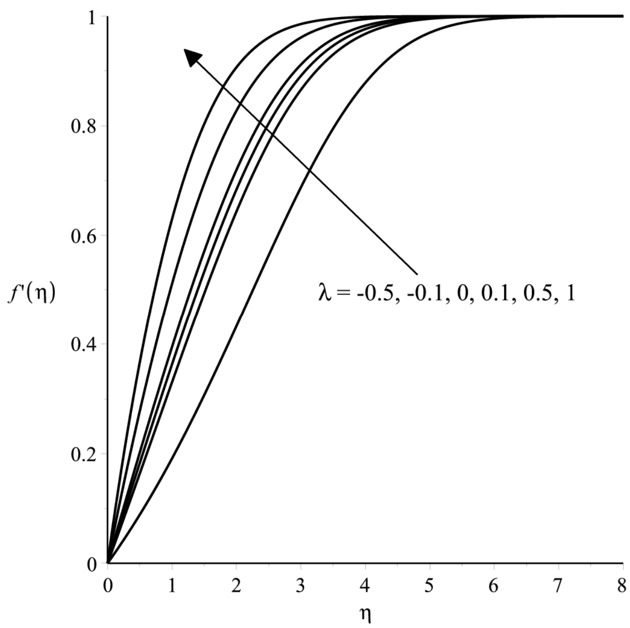

Figure 5. Velocity profiles $f'(\eta)$ for λ when $Ec = \phi_1 = 0.1,\ \phi_2 = 0.06$ and $\Pr = 6.2$.

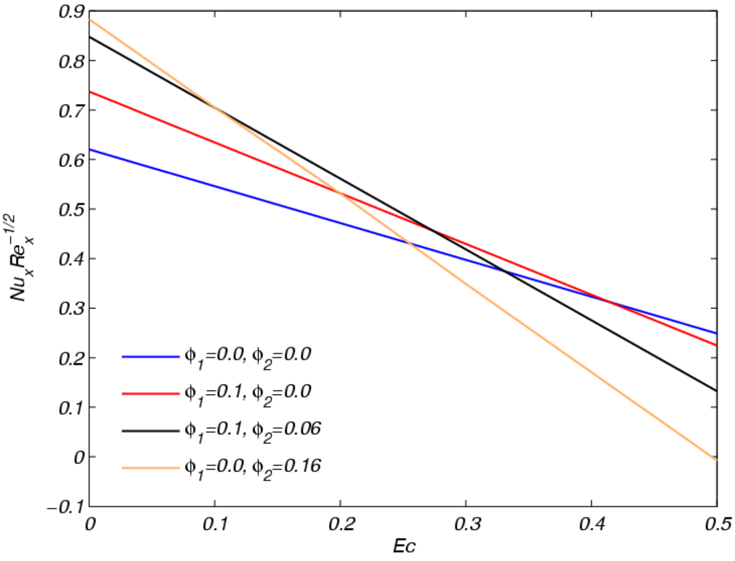

Figure 6. Distribution of $Nu_x \operatorname{Re}_x^{-1/2}$ for Ec when $\Pr = 6.2$ and $\lambda = 0$.

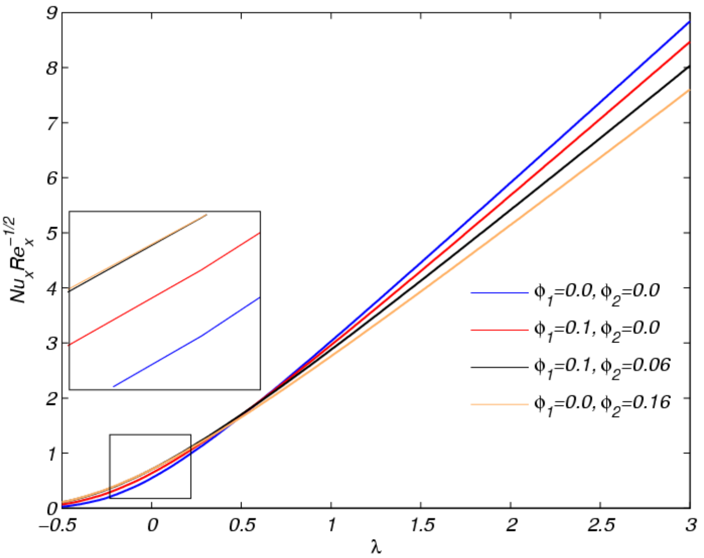

Figure 7. Distribution of $Nu_x \operatorname{Re}_x^{-1/2}$ for λ when $\Pr = 6.2$ and $Ec = 0.1$.

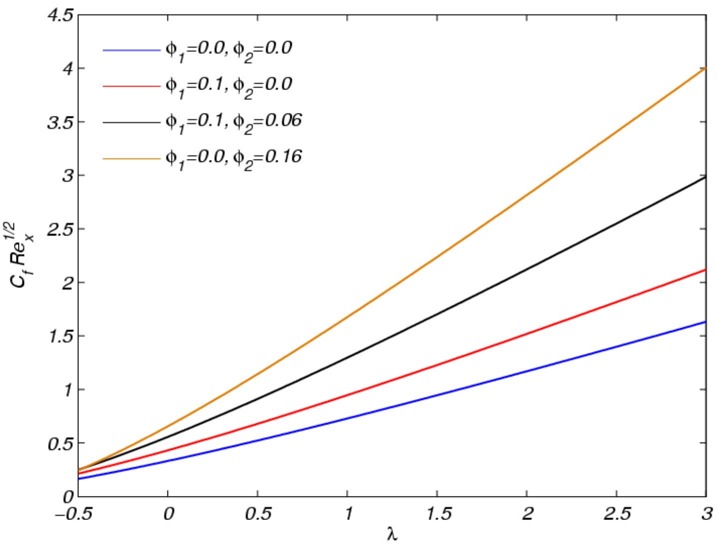

Figure 8. Distribution of $C_f \operatorname{Re}_x^{1/2}$ for λ when $\Pr = 6.2$ and $Ec = 0.1$.

CONCLUSION

As summary, it is found that the presence of viscous dissipation effect and the injection effect has enhanced the thermal boundary layer thickness while the suction effect reduced the thermal and the velocity boundary layer thicknesses. It is observed that high values of Ec may reduce the convective heat transfer capability to pure conduction. The suction effect results in the increase in reduced Nusselt number and the skin friction coefficient while the injection effect does contrary. Furthermore, the $Ag - Al_2O_3 \, / \, Water$ hybrid nanofluid tested in this study shows competitive results with the $Ag \, / \, Water$ nanofluid in certain cases. This shows the hybrid nanofluid potential in replacing the nanofluid especially with expensive nanomaterial like silver. The hybrid nanofluid provides well performance in the heat transfer capabilities along with the metal nanofluid but more economical in price since it is synthesized with cheap oxide nanomaterial.

ACKNOWLEDGEMENT

The authors would like to acknowledge the funding offered by the Ministry of Education Malaysia's Fundamental Research Grant Scheme (FRGS) under the grant number of FRGS/1/2019/STG06/UMP/02/1 (RDU1901124).

REFERENCES

[1] K. V. Wong and O. De Leon, "Applications of Nanofluids: Current and Future," Advances in Mechanical Engineering, vol. 2010, pp. 1-11, 2010.

[2] S. S. U. Devi and S. P. A. Devi, "Heat transfer enhancement of Cu - Al2O3/water hybrid nanofluid flow over a stretching sheet," Journal of the Nigerian Mathematical Society, vol. 36, pp. 419-433, 2017.

[3] S. S. Ghadikolaei, M. Yassari, H. Sadeghi, K. Hosseinzadeh, and D. D. Ganji, "Investigation on thermophysical properties of Tio2–Cu/H2O hybrid nanofluid transport dependent on shape factor in MHD stagnation point flow," Powder Technology, vol. 322, pp. 428-438, 2017/12/01/ 2017.

[4] Y. B. Kho, A. Hussanan, M. K. A. Mohamed, N. M. Sarif, Z. Ismail, and M. Z. Salleh, "Thermal radiation effect on MHD Flow and heat transfer analysis of Williamson nanofluid past over a stretching sheet with constant wall temperature," Journal of Physics: Conference Series, vol. 890, pp. 1-6, 2017.

[5] M. Sheikholeslami, "CuO-water nanofluid flow due to magnetic field inside a porous media considering Brownian motion," Journal of Molecular Liquids, vol. 249, pp. 921-929, 2018.

[6] H. T. Alkasasbeh, M. Z. Swalmeh, A. Hussanan, and M. Mamat, "Effects Of Mixed Convection On Methanol And Kerosene Oil Based Micropolar Nanofluid Containing Oxide Nanoparticles," CFD Letters vol. 11, pp. 55-68, 2019.

[7] W. Ibrahim and M. Negera, "MHD slip flow of upper-convected Maxwell nanofluid over a stretching sheet with chemical reaction," Journal of the Egyptian Mathematical Society, vol. 28, p. 7, 2020/01/20 2020.

[8] K. Muhammad, T. Hayat, A. Alsaedi, B. Ahmad, and S. Momani, "Mixed convective slip flow of hybrid nanofluid (MWCNTs + Cu + Water), nanofluid (MWCNTs + Water) and base fluid (Water): a comparative investigation," Journal of Thermal Analysis and Calorimetry, vol. 143, pp. 1523-1536, 2021/01/01 2021.

[9] T. Srinivasulu and B. S. Goud, "Effect of inclined magnetic field on flow, heat and mass transfer of Williamson nanofluid over a stretching sheet," Case Studies in Thermal Engineering, vol. 23, p. 100819, 2021/02/01/ 2021.

[10] H. Blasius, "Grenzschichten in flssigkeiten mit kleiner reibung," Zeitschrift für Angewandte Mathematik und Physik, vol. 56, pp. 1-37, 1908.

[11] B. C. Sakiadis, "Boundary layer behavior on continuous solid surfaces: I. Boundary layer equations for two dimensional and axisymmetric flow," American Institute of Chemical Engineers (AIChE) Journal, vol. 7, pp. 26-28, 1961.

[12] R. C. Bataller, "Radiation effects for the Blasius and Sakiadis flows with a convective surface boundary condition," Applied Mathematics and Computation, vol. 206, pp. 832-840, 2008.

[13] F. Aman, A. Ishak, and I. Pop, "MHD Stagnation Point Flow of a Micropolar Fluid Toward a Vertical Plate with a Convective Surface Boundary Condition," Bulletin of the Malaysian Mathematical Sciences Society, vol. 36, pp. 865-879, 2013.

[14] M. K. A. Mohamed, N. A. Z. Noar, M. Z. Salleh, and A. Ishak, "Mathematical Model of Boundary Layer Flow over a Moving Plate in a Nanofluid with Viscous Dissipation," Journal of Applied Fluid Mechanics, vol. 9, 2016.

[15] A. Jamaludin and R. Nazar, "Ingham problem for mixed convection flow of a nanofluid over a moving vertical plate with suction and injection effects," Sains Malaysiana, vol. 47, pp. 2213-2221, 2018.

[16] M. Qasim and B. Ahmad, "Numerical solution for the blasius flow in a casson fluid with viscous dissipation and convective boundary conditions," vol. 46, pp. 689-697, 2015.

[17] W. Khan, Z. Khan, and R. Haq, "Flow and heat transfer of ferrofluids over a flat plate with uniform heat flux," The European Physical Journal Plus, vol. 130, pp. 1-10, 2015.

[18] N. Ramli, S. Ahmad, and I. Pop, "Slip effects on MHD flow and heat transfer of ferrofluids over a moving flat plate," AIP Conference Proceedings, vol. 1870, p. 040015, 2017.

[19] A. Aziz, "A similarity solution for laminar thermal boundary layer over a flat plate with a convective surface boundary condition," Communications in Nonlinear Science and Numerical Simulation, vol. 14, pp. 1064-1068, 2009.

[20] A. Ishak, "Similarity solutions for flow and heat transfer over a permeable surface with convective boundary condition," Applied Mathematics and Computation, vol. 217, pp. 837-842, 2010.

[21] M. C. Raju, A. J. Chamkha, J. Philip, and S. V. K. Varma, "Soret effect due to mixed convection on unsteady magnetohydrodynamic flow past a semi infinite vertical permeable moving plate in presence of thermal radiation, heat absorption and homogenous chemical reaction," International Journal of Applied and Computational Mathematics, vol. 2, pp. 1-15, 2016.

[22] N. Anuar, N. Bachok, and I. Pop, "A stability analysis of solutions in boundary layer flow and heat transfer of carbon nanotubes over a moving plate with slip effect," Energies, vol. 11, p. 3243, 2018.
[23] A. Ahmed, J. I. Siddique, and M. Sagheer, "Dual solutions in a boundary layer flow of a power law fluid over a moving permeable flat plate with thermal radiation, Viscous Dissipation and Heat Generation/Absorption," vol. 3, p. 6, 2018.
[24] M. K. A. Mohamed, F. N. Abas, and M. Z. Salleh, "MHD boundary layer flow over a permeable flat plate in a ferrofluid with thermal radiation effect," Journal of Physics: Conference Series, vol. 1366, p. 012014, 2019.
[25] B. K. Jha and G. Samaila, "Thermal radiation effect on boundary layer over a flat plate having convective surface boundary condition," SN Applied Sciences, vol. 2, p. 381, 2020/02/11 2020.
[26] B. Gebhart, "Effects of viscous dissipation in natural convection," Journal of Fluid Mechanics, vol. 14, pp. 225-232, 1962.
[27] S. Ahmad, A. Rohni, and I. Pop, "Blasius and Sakiadis problems in nanofluids," Acta Mechanica, vol. 218, pp. 195-204, 2011/05/01 2011.
[28] Y. Yirga and B. Shankar, "MHD flow and heat transfer of nanofluids through a porous media due to a stretching sheet with viscous dissipation and chemical reaction effects," International Journal for Computational Methods in Engineering Science and Mechanics, vol. 16, pp. 275-284, 2015.